ACS OMEGA

http://pubs.acs.org/journal/acsodf

Article

Biogeochemical Assessment of the Coalbed Methane Source, Migration, and Fate: A Case Study of the Shizhuangnan Block, Southern Qinshui Basin

Yang Li, Jian Chen,* Shuheng Tang, Songhang Zhang, and Zhaodong Xi

Cite This: *ACS Omega* 2022, 7, 7715−7724

Read Online

ACCESS | Metrics & More | Article Recommendations

ABSTRACT: The exploration and exploitation of coalbed methane (CBM), an essential unconventional gas resource, have received much attention. In terms of shallow groundwater assessment during CBM production, biogenic methane natural formation in situ and methane migration from deep sources into shallow aquifers need to be of most concern. This study analyzes geochemical surveys including ions, isotopes, and dissolved methane concentrations in 75 CBM coproduced water samples in the southern Qinshui Basin. Most of these water samples are weakly alkaline. Some samples' negative oxidation/reduction potential (ORP) values reveal that the CBM reservoir water samples are mainly produced from reductive groundwater environments. Cl^-, Na^+, and HCO_3^- are the dominant ionic constituents of the water samples, which are usually associated with dissolved methane concentrations. The biogeochemical parameters and isotopic features provide an opportunity to assess the origin, migration, and oxidation of biogenic or thermogenic methane. Some water samples suggest biogenic methane formation in situ characterized by negligible SO_4^{2-} and NO_3^- concentrations and low $\delta^{13}C_{CH4}$. Only a few water samples indicate the migration of biogenic methane into shallow aquifers without oxidation based on elevated SO_4^{2-}, NO_3^-, and $\delta^{13}C_{DIC}$ and low $\delta^{13}C_{CH4}$. A few cases characterized by elevated $\delta^{13}C_{CH4}$, negative $\delta^{13}C_{DIC}$ values, and negligible SO_4^{2-} and methane concentrations suggest the oxidation of biogenic methane rather than the migration of thermogenic methane. A significant number of cases mean methane migration to shallow aquifers. Partial oxidation of thermogenic or mixed methane is evaluated by negligible SO_4^{2-}, NO_3^-, and methane concentrations and elevated $\delta^{13}C_{CH4}$. Dissolved methane isotopic compositions and aqueous biogeochemical features help study methane formation and potential migration in shallow groundwater.

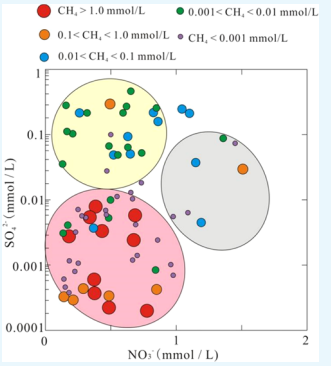

1. INTRODUCTION

The rapid development of drilling and hydraulic fracturing technologies has promoted the large-scale exploitation of coalbed methane (CBM).[1,2] Groundwater migration is the main reason for methane migration and accumulation.[3] The direct impact of groundwater transport on methane has attracted widespread attention, and methane transport significantly impacts water quality caused by CBM exploitation.[4] In general, elevated methane concentrations are mainly found in the Na−Cl and Na−HCO_3 groundwater types.[5] However, the analysis of groundwater biogeochemical characteristics to evaluate redox conditions can reveal whether methane is thermally or biologically formed and whether it is formed in situ or migrated from deep areas.

Determining the CBM source by its isotopic characteristics is essential, but isotopic fractionations caused by methane oxidation may affect CBM source identification.[6] Therefore, it is necessary to develop reliable methods to distinguish true thermogenic methane and pseudothermic methane and demonstrate methane migration from deep geological formations to shallow ones. Biogenic methane formation requires a high degree of reductive environment, meaning that methanogens produce methane after oxygen, nitrate, and sulfate are consumed. The analysis of the coupling relationship within biogeochemical parameters can provide a significant basis for the possibility of biogenic methane formation in situ. Furthermore, the carbon and hydrogen isotopic characteristics of biogenic methane are different from those of thermogenic methane,[7] and isotopic analyses of dissolved inorganic carbon ($\delta^{13}C_{DIC}$), nitrate ($\delta^{15}N_{NO3}$, $\delta^{18}O_{NO3}$), and sulfate ($\delta^{34}S_{SO4}$, $\delta^{18}O_{SO4}$) provide a vital complement to the study of aquifer redox environments for methane formation and migration.[8] Therefore, a comprehensive analysis of groundwater biogeochemistry and isotopes can make it possible to determine the origin and migration of methane.

The Qinshui Basin is one of China's earliest CBM commercial development zones, which has considerable coal

Received: November 18, 2021
Accepted: February 11, 2022
Published: February 22, 2022

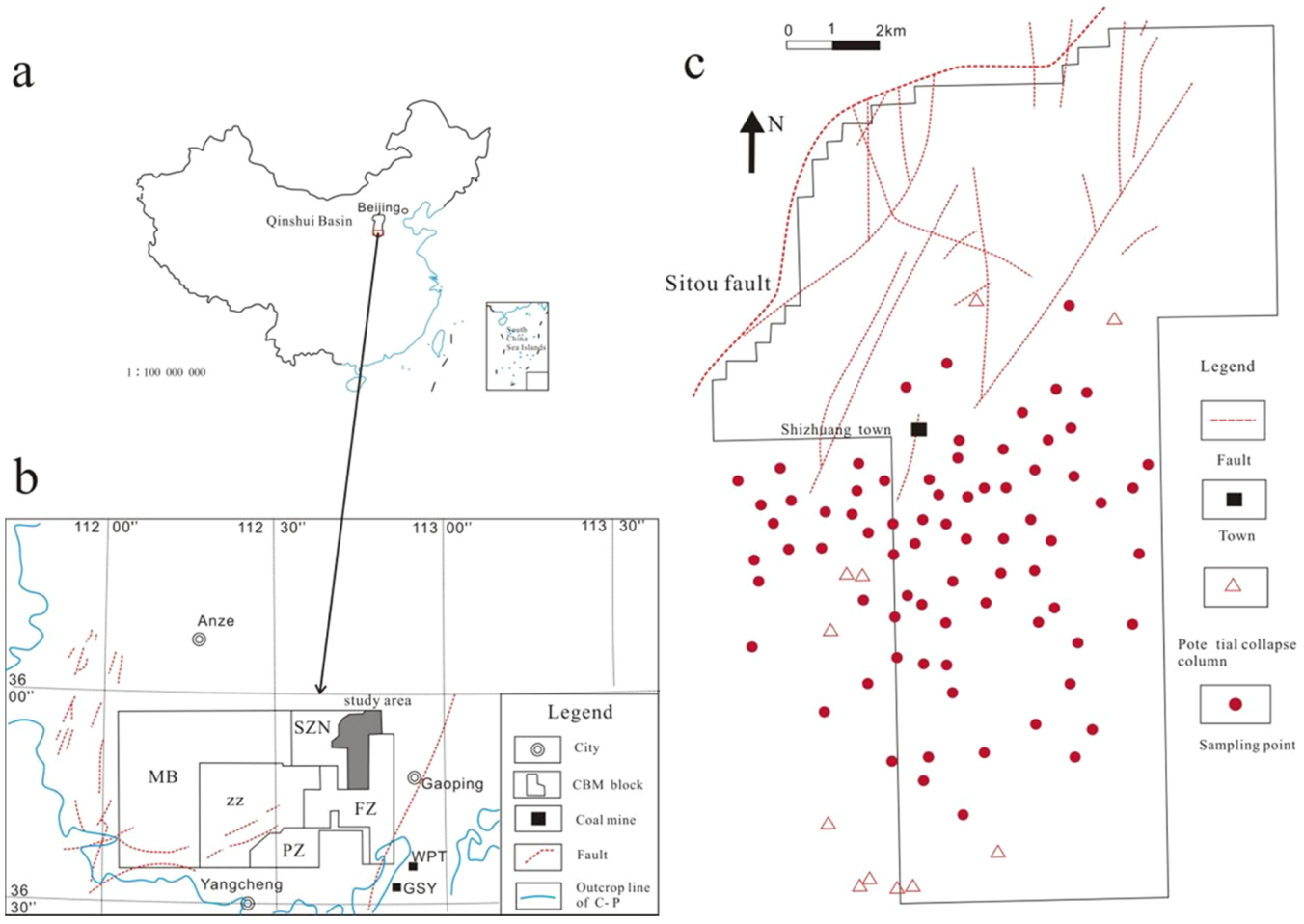

Figure 1. (a) Location of the Qinshui Basin in China; (b) location of the Shizhuangnan block in the southern Qinshui Basin of China (FZ: the Fanzhuang block; MB: the Mabi block; PZ: the Panzhuang block; SZN: the Shizhuangnan block; ZZ: the Zhengzhuang block); and (c) main structure diagram and CBM wells for the study in the Shizhuangnan block.

and CBM resources. The Shanxi Formation and Taiyuan Formation are the primary sources of CBM exploration and development. In the mid-1990s, most coalbed methane exploration took off with the advance of mining technology and infrastructure. The Shizhuangnan block is an essential commercial CBM development block in the Qinshui Basin.[9] This study aims to determine the source or migration of coalbed methane by describing redox processes in shallow groundwater environments of the Shizhuangnan block. This method takes advantage of the general laws governing the methane source, migration, and fate and can be transferred to other CBM reservoir studies.

2. GEOLOGICAL BACKGROUND

Qinshui Basin, located in the southeastern Shanxi province, is a large complex synclinal basin formed on the late Paleozoic basement (Figure 1a). The coal resources in the Qinshui Basin are mostly bituminous and anthracite from Carboniferous to Permian. Hence, Qinshui Basin has excellent conditions to exploit coalbed methane resources, which is the first and largest coalbed methane commercial development basin in China.[10,11] The south of Qinshui Basin is a high investment and research area of CBM exploration and development. The CBM production of the southern Qinshui Basin accounts for more than 90% of the total yield of the Qinshui Basin. The Shizhuangnan block is located in the northwest dipping slope belt in the southern Qinshui Basin (Figure 1b). The tectonic movement has a significant influence on the tectonic morphology of this area. The overall structural characteristics of the Shizhuangnan block are relatively simple, and the overall topography gradually tilts from southeast to northwest.[12] The most significant Sitou fault in the northwest area is a normally closed fault extending from northeast to southwest (Figure 1c). In the southern part of the Sitou fault, the distance and dip angle gradually become smaller, and there are some hidden minor faults around. The Sitou fault has poor water connectivity, which is significant to CBM reservoir formation in the study area.[13]

The exploration and development of CBM in the Shizhuangnan block is the No. 3 coal seam of Shanxi Formation and No. 15 coal seam of Taiyuan Formation, which are large and stable minable seams. The No. 3 coal seam roof is mainly composed of mudstone and sandy mudstone, while the floor is mainly composed of siltstone and mudstone. The No. 3 coal seam in the Shizhuangnan block has a wide range and stable distribution, located in the lower part of the Shanxi Formation. The average thickness of the No. 3 coal seam used in the study area is 6 m, and the total buried depth is about 450−900 m. The overall coal seam shape shows a trend of shallowness in the southeast and depth in the northwest.[8,14] In this study, the No. 3 coal seam is the primary source of samples.

https://doi.org/10.1021/acsomega.1c06496
ACS Omega 2022, 7, 7715−7724

Due to the difference in the occurrence form and storage space, each type of aquifer is different in hydraulic connection and dynamic change. According to the difference of reservoir space, the aquifer in the south of the Qinshui Basin is divided into aquifer types. The sandstone fissured confined water aquifer of the Shanxi Formation is deeply buried in the lower Permian strata, which is the primary source of the No. 3 coal seam in the south of the Qinshui Basin (Figure 2). The No. 3 coal seam is a weakly confined aquifer between sandstone water layers, belonging to a solid water-rich aquifer. On the regional scale, the hydrogeological conditions of the Shizhuangnan block are relatively simple. Overall, the Shizhuangnan block can be approximated as a west-dipping monoclinal structure. Stable aquifers are formed between each aquifer, and there is no vertical hydraulic connection between these aquifers, creating an independent coal aquifer system. The groundwater in the Shizhuangnan block is deeply buried, and its runoff is slow under gravity action. The exposed part of the Jinhuo fault zone on the basin's eastern edge is high, and the coal reservoir is replenished after receiving atmospheric precipitation and surface runoff. Sitou fault on the west forms a natural barrier of the underground reservoir. CBM is blocked under hydrostatic pressure, leading to high reservoir pressure. The retention area has good sealing and gas-bearing properties, which is conducive to the storage of CBM.

3. RESULTS AND DISCUSSION

3.1. Geochemical Characteristics of the CBM Reservoir Water of the Shizhuangnan Block. The geochemical properties of the CBM coproduced water samples in the Shizhuangnan block include pH, ORP, main ionic parameters, and isotopic characteristics. Main ionic parameters, pH, and ORP were tested for all 75 water samples. The pH values of these collected water samples range from 7.2 to 8.9, suggesting that the reservoir water is alkaline in the Shizhuangnan block. The ORP values vary from −141 to 184 and differ among various areas in the study block, affected by the reservoir redox environments. In total, 50 CBM coproduced water samples have ORP positive values, while 25 water samples have negative ORP values. Negative ORP values generally mean reductive reservoir conditions, while positive values suggest oxidized reservoir environments. Dissolved methane concentrations of all water samples were determined from the Shizhuangnan block. These methane concentrations were measured above the detection limit, but it has a wide value range from 0.0001 to 1 mmol/L. Elevated dissolved methane concentrations related to negative ORP reveal that the majority of the highest concentrations of methane were saved predominantly under the reductive reservoir conditions (Figure 3).

Ion compositional characteristics reveal that Na^+, Cl^-, and HCO_3^- account for a vast proportion of the significant anions in the Shizhuangnan block. The average concentrations of Na^+, Cl^-, and HCO_3^- are 15.71, 8.50, and 6.03 mmol/L, respectively. The majority of SO_4^{2-} concentrations are commonly lower than other ions, while NO_3^- concentrations are relatively high with a range from 0.10 to 1.60 compared with SO_4^{2-}. With the flow of coal seam water, water−rock interactions and microbial action change the concentrations of some ions, resulting in the depletion of SO_4^{2-} and NO_3^- and the increase in Na^+, Cl^-, and HCO_3^-.[15,16]

Dissolved methane concentrations can be correlated with different geochemical data from the CBM coproduced water samples (Figure 4a,b). The first type with low Na^+, Cl^-, and HCO_3^- concentrations meaning freshwater near the original point has low methane concentrations. The second groundwater type with low Cl^- and high Na^+ and HCO_3^- concentrations has low methane concentrations. The samples of this type seem to be affected by cation exchange, resulting in increased Na^+ and HCO_3^-.[17] These samples are mainly located

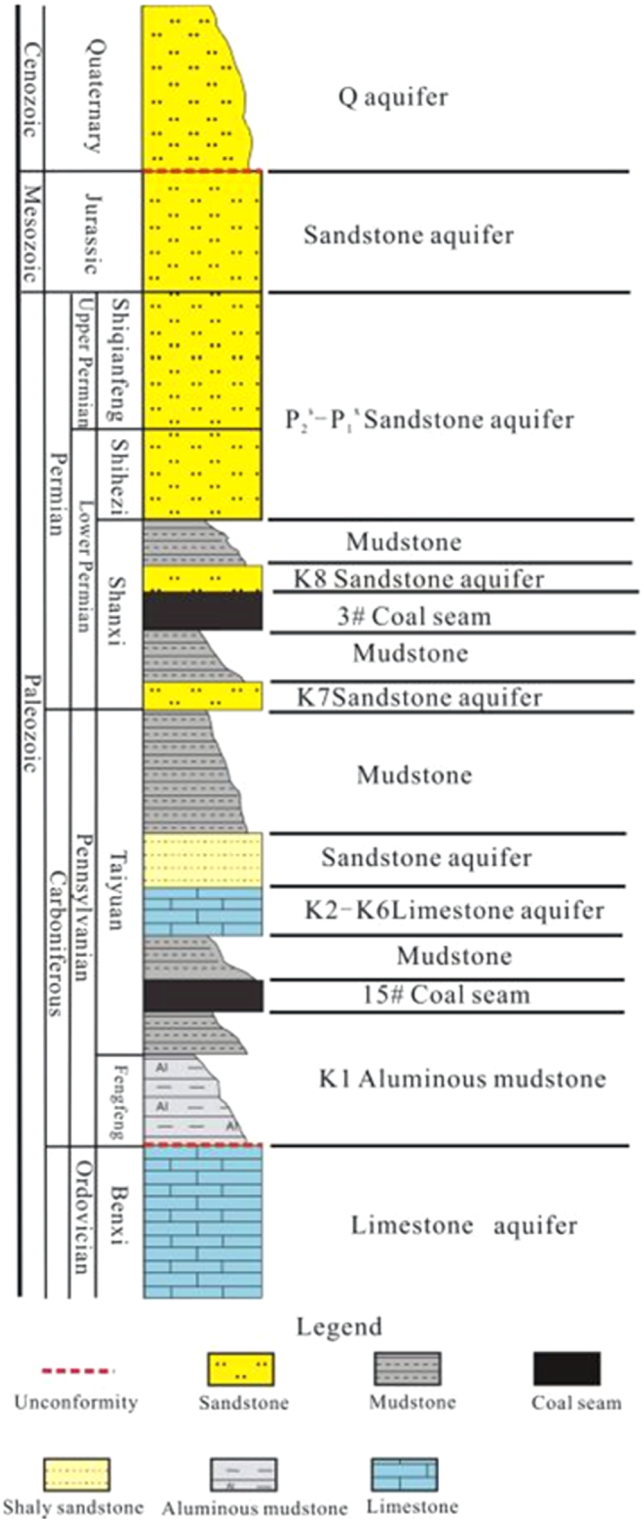

Figure 2. Schematic diagram of the aquifer and strata of the southern Qinshui Basin.

https://doi.org/10.1021/acsomega.1c06496
ACS Omega 2022, 7, 7715−7724

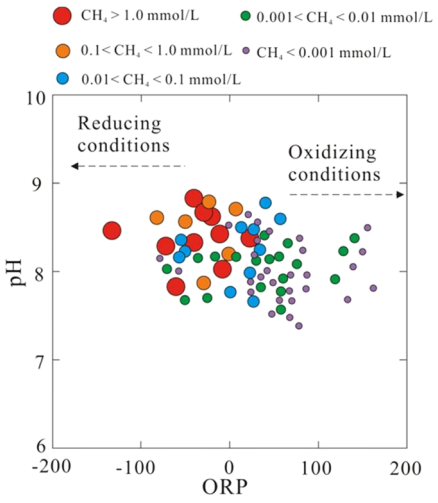

Figure 3. Plot of ORP and pH versus dissolved methane concentrations indicated by the size and color of symbols in the CBM coproduced water samples from the No. 3 coal seam.

in the central and western parts of the Shizhuangnan block. The third type of groundwater samples with high Na^+, Cl^-, and HCO_3^- concentrations has elevated methane concentrations following other studies in other CBM reservoirs.[5,7,10] Therefore, to further identify the occurrence environments of methane in CBM reservoir water, the following geochemical indicators are used to characterize it.

3.2. Biogeochemical Parameters and Redox Environments of Methane Occurrence. Several biogeochemical parameters are used to characterize the metabolic activities of different microorganisms to study the CBM reservoir redox conditions for methane production, migration, and storage.[18] Methane oxidative reactions may occur when methane migrates to groundwater with better oxidative conditions. A series of redox reactions, including denitrification, manganese and iron reduction, reduction of bacterial sulfate, and methane formation, occur successively as the groundwater environments transition from oxidative conditions to reductive conditions. For example, when the primary oxidant in groundwater is sulfate, the methane oxidation process is accompanied by bacterial sulfate reduction. Microorganisms mediate the process, called anaerobic oxidation methane (AOM) and bacterial sulfate reduction (BSR). With the consumption of oxidants, the relative reductive environments are conducive to methanogen metabolism and biogenic methane production in situ.[19,20]

Most samples with ORP more than 0 contain negligible dissolved methane concentrations (Figure 3). It is impossible to generate biogenic methane in situ in a relatively oxidized groundwater environment. Only a few samples with high ORP values dissolve a certain amount of methane, resulting from methane migration from other areas.[21] There is a negative correlation between NO_3^- contents and methane concentrations in groundwater samples because groundwater environments containing high NO_3^- are not suitable for methane preservation (Figure 5). Similarly, there is a negative

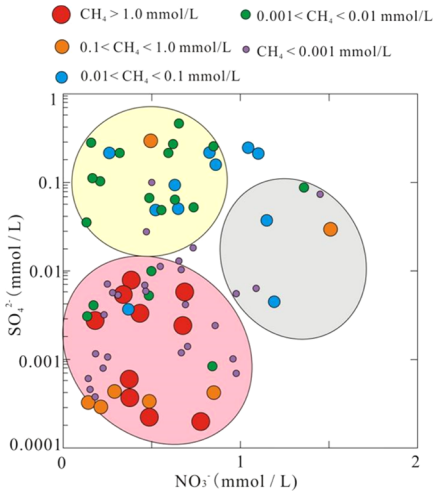

Figure 5. Plot of NO_3^- and SO_4^{2-} versus dissolved methane concentrations indicated by the size and color of symbols in the CBM coproduced water samples from the No. 3 coal seam.

correlation between SO_4^{2-} contents and methane concentrations. It can be inferred that the presence of elevated methane in groundwater is not apparent until SO_4^{2-} concentrations are less than 0.01 mmol/L. When methane migrates into aquifers containing O_2, SO_4^{2-}, or NO_3^-,

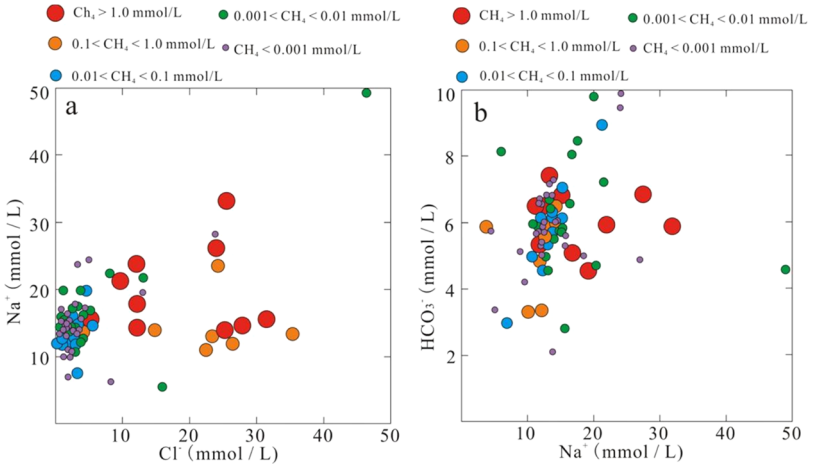

Figure 4. (a) Plot of Cl^- and Na^+ versus dissolved methane concentrations and (b) plot of Na^+ and HCO_3^{2-} versus dissolved methane concentrations indicated by the size and color of symbols in the CBM coproduced water samples from the No. 3 coal seam.

https://doi.org/10.1021/acsomega.1c06496
ACS Omega 2022, 7, 7715−7724

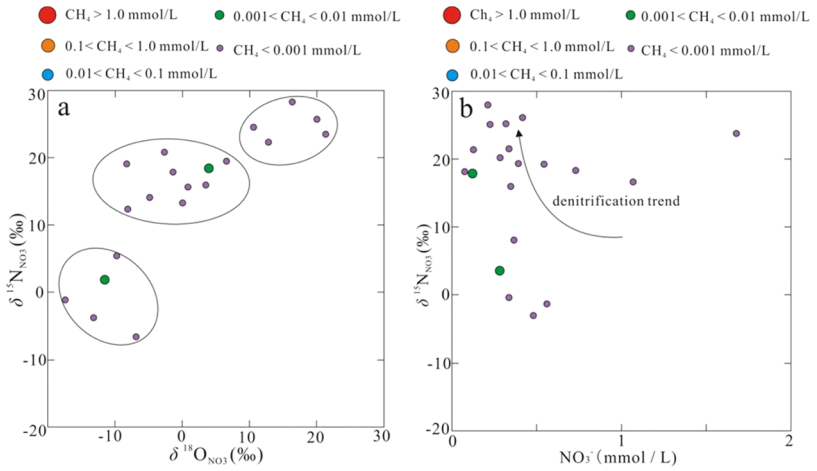

Figure 6. (a) Plot of $\delta^{18}O_{NO3}$ and $\delta^{15}N_{NO3}$ versus dissolved methane concentrations and (b) plot of NO_3^- and $\delta^{15}N_{NO3}$ versus dissolved methane concentrations indicated by the size and color of symbols in the CBM coproduced water samples from the No. 3 coal seam.

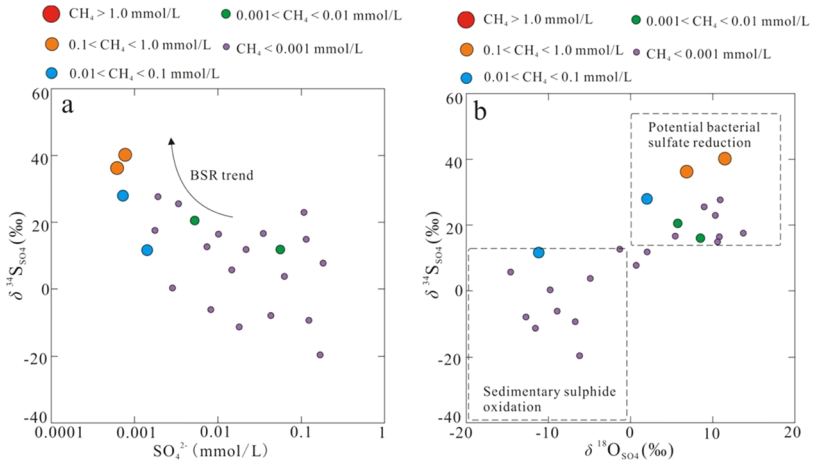

Figure 7. (a) Plot of SO_4^{2-} and $\delta^{34}S_{SO4}$ versus dissolved methane concentrations and (b) plot of $\delta^{18}O_{SO4}$ and $\delta^{34}S_{SO4}$ versus dissolved methane concentrations indicated by the size and color of symbols in the CBM coproduced water samples from the No. 3 coal seam.

relatively reductive conditions may be formed after these oxidizers are consumed.[22] The redox ladder concept further explains these analysis results (Figure 5).

Figure 5 reveals the coupling relationship between NO_3^- and SO_4^{2-} concentrations and dissolved methane concentrations. The first groundwater sample type with high NO_3^- concentrations (>1 mmol/L) and moderate sulfate concentrations (0.001−0.1 mmol/L) contains only a small amount of dissolved methane characterized by a light gray circle. The elevated NO_3^- and SO_4^{2-} concentrations represent that neither complete denitrification nor complete bacterial sulfate reduction took place in the groundwater conditions. Accordingly, the formation of biogenic methane in situ is restricted. In this type of groundwater sample, only one sample has elevated methane concentrations ($0.1 < CH_4 < 1.0$ mmol/L), which is associated with the migration of methane to aquifers containing elevated NO_3^- and SO_4^{2-}. The second groundwater sample type has high SO_4^{2-} (>0.01 mmol/L), low NO_3^- (<1 mmol/L), and negligible dissolved methane concentrations, except for one groundwater sample ($0.1 < CH_4 < 1.0$ mmol/L), which is characterized by the light yellow circle. It may be due to methane migration into these aquifers and partial oxidation through denitrification or BSR.[23] The last groundwater sample type contains negligible NO_3^- and SO_4^{2-} concentrations corresponding to these samples with the highest methane concentrations (light red circle). Therefore, the reservoir environments with the complete occurrence of BSR and denitrification are beneficial to methane preservation.[22]

3.3. Isotopic Characteristics in the CBM Water Reservoir of the Shizhuangnan Block. *3.3.1. Nitrogen and Oxygen Isotope Ratios of Nitrate in the CBM Water Reservoir of the Shizhuangnan Block.* Isotopes of NO_3^-, SO_4^{2-}, DIC, and methane are used to explain redox processes such as denitrification. Just 20 water samples have been measured for nitrate isotopes. The $\delta^{15}N_{NO3}$ values range from −3.9 to 29.1‰, while $\delta^{18}O_{NO3}$ values range from −18.4 to 22.8‰. The water source can be obtained by nitrogen and oxygen isotope ratios of nitrate.[24,25] A water sample kind characterized by relative low $\delta^{18}O_{NO3}$ values (<0‰) and low $\delta^{15}N_{NO3}$ (<10‰) with low NO_3^- concentrations demonstrates that NO_3^- is thought to result from the nitrification of organic matter (Figure 6a,b). This kind of groundwater is dominated by the lowest methane concentrations, except for one sample with methane concentrations between 0.001 and 0.01 mmol/L. Another kind of groundwater with relatively high $\delta^{15}N_{NO3}$ (>10‰) and low $\delta^{18}O_{NO3}$ ($-10‰ < \delta^{18}O_{NO3} < 10‰$) accompanied by relatively high NO_3^- concentrations likely

https://doi.org/10.1021/acsomega.1c06496
ACS Omega 2022, 7, 7715−7724

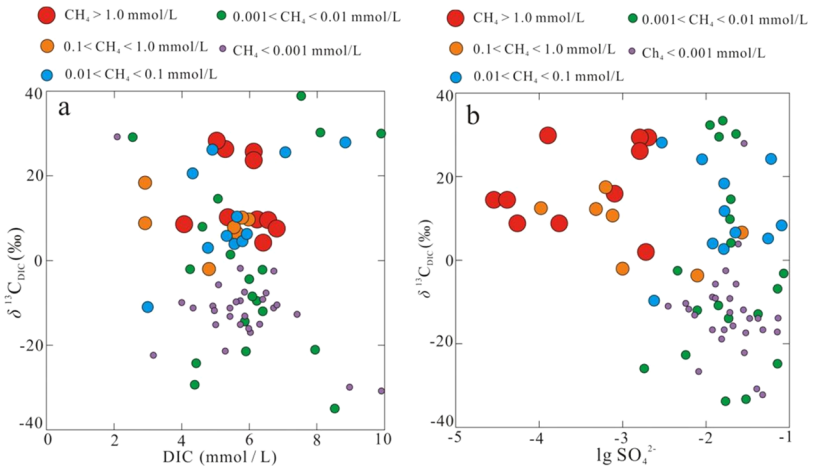

Figure 8. (a) Plot of DIC and $\delta^{13}C_{DIC}$ versus dissolved methane concentrations and (b) plot of lg SO_4^{2-} and $\delta^{13}C_{DIC}$ versus dissolved methane concentrations indicated by the size and color of symbols in the CBM coproduced water samples from the No. 3 coal seam.

results from manure spreading. These samples almost have negligible methane (<0.001 mmol/L) associated with different groundwater sources. The last kind of water is characterized by high $\delta^{18}O_{NO3}$ (>10‰) and $\delta^{15}N_{NO3}$ (>20‰) with negligible NO_3^- and methane concentrations. Theoretically, this isotopic signature could be derived from mineral fertilizers. In the process of denitrification, with the decrease of NO_3^- concentration, the residual NO_3^- gradually enriched in ^{15}N and ^{18}O. It can be seen that these samples may be affected by denitrification (Figure 6b).[26,27] Thus, nitrate isotopes reveal the various nitrate origins accompanied by little sign of denitrification depending on these isotopic analyses.

3.3.2. Sulfur and Oxygen Isotope Ratios of Sulfate in the CBM Water Reservoir of the Shizhuangnan Block. In the process of BSR, SO_4^{2-} concentrations are expected to decline, while ^{34}S and ^{18}O gradually accumulate in the residual SO_4^{2-}. The water samples with the highest SO_4^{2-} are companied with $\delta^{34}S_{SO4}$ between 20 and −20‰ (Figure 7a). Furthermore, $\delta^{18}O_{SO4}$ values (<0‰) indicate that the sulfate in these samples mainly comes from pyrite oxidation (Figure 7b), and some water samples associated with relatively low SO_4^{2-} concentrations usually have low $\delta^{34}S$ and $\delta^{18}O$, suggesting that sulfate comes from sulfide mineral oxidation.[28] The elevated $\delta^{34}S_{SO4}$ trend with gradually decreasing SO_4^{2-} indicates that BSR has occurred under the groundwater conditions (Figure 7a). Some samples with BSR evidence contain high dissolved methane concentrations.

3.3.3. Carbon Isotopic Compositions of Inorganic Carbon in the CBM Water Reservoir of the Shizhuangnan Block. The $\delta^{13}C_{DIC}$ values vary from −36.0 to 38.8 in the groundwater samples. $\delta^{13}C_{DIC}$ is a critical evaluation parameter for methanogenesis and dissolved methane concentrations. Elevated methane concentrations are usually associated with high $\delta^{13}C_{DIC}$ values. The isotopic characteristics of dissolved inorganic carbon (DIC) indicate the carbon source of DIC and the process of producing or influencing DIC. The negative $\delta^{13}C$ values reveal that DIC comes from carbonate dissolution and organic matter oxidation.[29] These $\delta^{13}C$ values are associated with low methane concentrations (Figure 8a). The positive $\delta^{13}C$ values mean the occurrence of methanogenesis in groundwater environments because methanogens preferentially utilize ^{12}C, resulting in the remaining ^{13}C enriched in DIC. These samples have relatively high dissolved methane concentrations.[30]

The water samples of high SO_4^{2-} concentrations are associated with low $\delta^{13}C_{DIC}$ values (Figure 8b). Moreover, the water samples with the lowest SO_4^{2-} concentrations are associated with the highest $\delta^{13}C_{DIC}$ values and elevated methane concentrations. This assumption confirms that BSR needs to be completed before methanogenesis in the coal reservoir water environments.[31,32]

3.4. Methane Formation, Migration, and Oxidation in Coal Reservoir Water. Isotopic distributions of methane and carbon dioxide often reflect the effects of methane formation, fractionation, and oxidation[33] (Figure 9). These isotopic characteristics of methane and carbon dioxide differ among different blocks in the study area.[10] Furthermore, the redox parameters are sufficient in the study area, including ORP, pH, main ions, and DIC, sulfate, and nitrate isotopic characteristics. Combined with the abovementioned analysis, the biogeochemical conditions for methane formation, migration, and oxidation can be evaluated.[3,10,18]

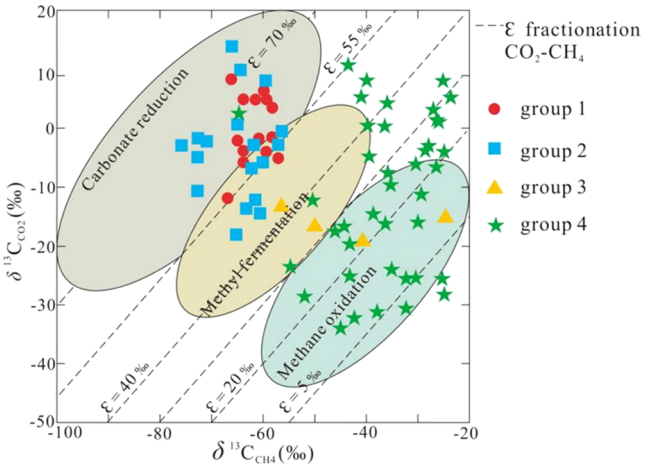

Figure 9. Plot of $\delta^{13}C_{CH4}$ and $\delta^{13}C_{CO2}$ represent methane formation and consumption containing four groups of the CBM coproduced water samples in the No. 3 coal seam.

3.4.1. Biogenic Methane Generation (Group No. 1). As shown in Table 1, group No. 1 with characteristics of $\delta^{13}C_{CH4}$

https://doi.org/10.1021/acsomega.1c06496
ACS Omega 2022, 7, 7715−7724

Table 1. Categories Classification, Methane Type, and Biogeochemical Characteristics[a]

category	group no. 1	group no. 2	group no. 3	group no. 4
N	12	19	4	40
$\delta^{13}C_{CH4}$ (‰)	< −55	< −55	> −55	> −55
methane	high	relatively high	low	relatively low
NO_3^-	negligible	relatively high	low	negligible
SO_4^{2-}	negligible	relatively high	low	negligible
$\delta^{13}C_{DIC}$	positive	negative	negative	
CH_4 type	A	B	C	D
redox conditions	reductive	oxidized	oxidized	relatively reductive
proportion (%)	18	25	5	52

[a]A: biogenic methane in situ. B: biogenic methane migrated into more oxidized environments without oxidation. C: biogenic methane migrated into more oxidized environments. D: thermogenic methane or mixed methane origin.

(<−55‰) suggests the biogenic methane source. Negligible NO_3^- and SO_4^{2-} concentrations of geochemical signatures indicate that 12 of 75 methane in group No. 1 originated from methanogenesis. The other 63 water samples may have undergone migration and/or oxidation.

3.4.2. Biogenic Methane Migrated to More Oxidized Aquifers (Group No. 2). Group No. 2 includes 19 water samples characterized by low $\delta^{13}C_{CH4}$ values (<−55‰) and relatively high SO_4^{2-} concentrations (>0.01 mmol/L) and NO_3^- concentration (>1 mmol/L). The methane isotopic characteristics do not agree with geochemical parameters, suggesting that in situ biogenic methane migrated from reductive aquifers to oxidized aquifers with no oxidation.[3] The $\delta^{13}C_{DIC}$ values for methane oxidation are consistent with the expected values because there is no evidence of methane oxidation, which may be due to the short residence time, the microbial anaerobic methane oxidation, and the relatively slow turnover of methane oxidation (Table 1).

3.4.3. Shallow Methane Aquifer of Apparent or Pseudothermogenic Methane (Group No. 3). The four water samples of group No. 3 characterized by $\delta^{13}C_{CH4}$ values (>−55‰) suggest the thermogenic methane source or methane oxidation. The elevated $\delta^{13}C_{CH4}$ values are usually associated with low $\delta^{13}C_{DIC}$, SO_4^{2-}, and elevated $\delta^{34}S_{SO4}$ values. It is supposed that biogenic methane oxidation by BSR is the primary cause rather than thermogenic methane from deeper aquifers. The ^{13}C in the remaining methane is enriched in the process, resulting in a relatively high $\delta^{13}C$ value, which may be misunderstood as a characteristic of thermogenic methane.[18,34] As shown in Table 1, the carbon isotopes of methane and DIC, $\delta^{34}S_{SO4}$, and low methane concentrations further prove methane oxidation. Therefore, it is presumed that the water samples in group No. 3 are either influenced by methane oxidation or analytical uncertainty resulting from low methane concentrations rather than thermogenic methane migration from deeper aquifers.

3.4.4. Biogenic−Thermogenic Mixed Methane (Group No. 4). Group No. 4 includes 40 water samples characterized by negligible SO_4^{2-} and NO_3^-, and these samples are associated with relatively low methane concentrations and high $\delta^{13}C_{CH4}$ (>−55‰) (Table 1). It is supposed that thermogenic methane or mixed biogenic and thermogenic methane has migrated to shallow aquifers and has partially oxidized (Figure 9).

3.5. Carbon Isotope Variation in Methane and Dissolved Inorganic Carbon. The isotopic characteristics of methane and carbon dioxide provide a tool for studying microbial oxidation of methane.[35,36] The biological oxidation of methane causes significant changes in methane and carbon dioxide isotopic characteristics. It is because microorganisms preferentially utilize ^{12}C in methane, resulting in ^{13}C enrichment in residual methane and ^{13}C enrichment in residual carbon dioxide.[37,38] The C and H isotopic patterns of dissolved methane in four sites affected by methane oxidation show a continuous and increasing enrichment with a slope of the oxidation trend (Figure 10a). The slope is 7‰, suggesting that every permil $\delta^{13}C_{CH4}$ value variation approximately causes 7‰ $\delta^{2}H_{CH4}$ variation.

There is a clear relationship in carbon isotope separation between methane and the coexistence of carbon dioxide during the biogenic methane oxidation process. Carbon isotope fractionation factors are written as $\alpha^{13}C_{CO2-CH4} = (\delta^{13}C_{CO2} + 1000)/(\delta^{13}C_{CH4} + 1000)$ in the biogenic methane oxidation process. The carbon isotopes $\delta^{13}C_{CH4}$ and $\delta^{13}C_{CO2}$ were collected from the abovementioned four wells (Figure 10b). The three lines represent isotopic fractionations of 0.985, 1.005, and 1.030, respectively.[39,40] The relatively low $\alpha^{13}C_{CO2-CH4}$ results and depleted $\delta^{13}C_{CO2}$ values of these wells in the study area result from extensive methane oxidation and production of ^{12}C in DIC.[41,42]

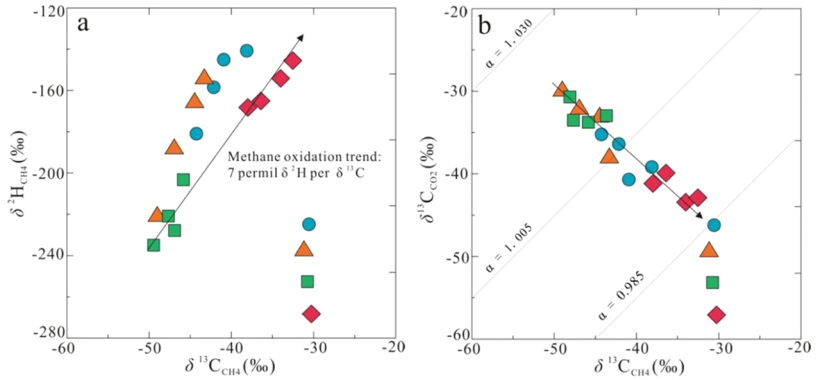

Figure 10. (a) Characteristics ^{13}C and ^{2}H of dissolved methane over time and (b) characteristics ^{13}C of dissolved CH_4 and CO_2 reveal oxidation trends in several wells from the No. 3 coal seam.

https://doi.org/10.1021/acsomega.1c06496
ACS Omega 2022, 7, 7715−7724

4. CONCLUSIONS

This study aims to determine the methane source, migration, and oxidation in the Shizhuangnan block by integrating isotopic parameters and biogeochemical data of dissolved methane and aqueous species. Identifying redox processes such as AOM and BSR is essential for determining methane occurrence in subsurface aquifers. The oxidation of biogenic methane in groundwater usually results in pseudothermogenic carbon isotopes, which may be misinterpreted as thermogenic methane intrusion from deep reservoirs. Therefore, it is inaccurate to differentiate the methane formation solely based on methane isotopic features. This study uses the concentrations and isotopes of dissolved methane and isotopic compositions of DIC, sulfate, and nitrogen to resolve potential ambiguities of the thermogenic methane source or biogenic methane oxidation. Low $\delta^{13}C_{CH4}$ values (<−55‰) accompanied with negligible NO_3^- and SO_4^{2-} concentrations provide clear evidence for methanogenesis in situ. Low $\delta^{13}C_{CH4}$ values (<−55‰) combined with high NO_3^- and SO_4^{2-} concentrations and high $\delta^{13}C_{DIC}$ reveal that biogenic methane migrated into more oxidized aquifers without oxidation. The samples with high $\delta^{13}C_{CH4}$ values (>−55‰) and low $\delta^{13}C_{DIC}$ values (<5) coexisting with negligible SO_4^{2-} and methane concentrations suggest oxidation rather than pseudothermogenic methane. Elevated $\delta^{13}C_{CH4}$ values (>−55‰) and low methane concentrations combined with negligible NO_3^- and SO_4^{2-} concentrations can result from mixed methane oxidation. Therefore, quantification of the extent of methane oxidation determines the methane origin in groundwater environments. The method developed in this study can be extended to other unconventional natural gas development areas worldwide.

5. MATERIALS AND METHODS

This study selected 75 coalbed methane wells with regular long-term drainage in the No. 3 coal seam from the Shizhuangnan block. For sustainable and effective CBM exploitation, all wells are located away from collapse columns and faults. Before CBM coproduced water sampling, sterilized polyethylene containers with sufficient 5 L volumes were made available for all testing and flushed more than three times with the coproduced water samples. During the water sampling process, the samples were directly collected from the outlets of the CBM wells with filter paper to remove solid residues. There is no contact between these outlets and the sampling bottles. The entire bottle was filled with water and closed using a lid immediately during the collection process. To avoid the influence of residual water in the drainage pipe, water samples were collected from CBM wells with stable water flow. Before being transferred to the laboratory, the water samples were stored in an incubator within 1−5 °C.

A total of 91 samples from these 75 wells were determined for main ions and isotopic parameters containing Cl^-, HCO_3^{2-}, Na^+, NO_3^-, SO_4^{2-}, dissolved inorganic carbon (DIC), dissolved methane, and isotopic compositions for carbon, hydrogen, oxygen, and nitrogen. Some wells were sampled repeatedly at regular intervals to assess water quality change over time. The sampling well locations used for this study are distributed in the central and western part of the Shizhuangnan block (Figure 1c). To collect representative data of aquifer environments, pH and oxidation/reduction potential (ORP) were measured in the field.

The filtered samples were chemically analyzed for main ions in the laboratory, and the samples were acidified to pH < 2 for cationic analysis. The analytical instruments used for the concentrations of cations and anions are inductively coupled plasma atomic emission spectroscopy (ICP-AES) and ion chromatography (IC), respectively. Furthermore, the compositions of dissolved gas were determined by gas chromatography. The isotopes of DIC ($\delta^{13}C_{DIC}$), NO_3^- ($\delta^{15}N_{NO3}$, $\delta^{18}O_{NO3}$), SO_4^{2-} ($\delta^{34}S_{SO4}$, $\delta^{18}O_{SO4}$), dissolved methane ($\delta^{13}C_{CH4}$, $\delta^{2}H_{CH4}$), and ($\delta^{13}C_{CO2}$, $\delta^{18}O_{CO2}$) were analyzed on a ThermoFisher MAT 253 isotope ratio mass spectrometer coupled to a Trace GC Ultra and GC Isolink. Stable isotopes were recorded in the internationally accepted delta notation (‰) relative to VPDB for $\delta^{13}C$ values, VSMOW for $\delta^{2}H$ and $\delta^{18}O$ values, VCDT for ^{34}S values, and N_2 in the air for $\delta^{15}N$ values. The reliability of test results was determined by repeated analysis of select samples from some wells.

AUTHOR INFORMATION

Corresponding Author

Jian Chen − *School of Earth and Environment, Anhui University of Science and Technology, Huainan 232001 Anhui, China; State Key Laboratory of Mining Response and Disaster Prevention and Control in Deep Coal Mines, Anhui University of Science & Technology, Huainan 232001 Anhui, China*; orcid.org/0000-0003-3864-8737; Email: cscchenjian@163.com

Authors

Yang Li − *School of Earth and Environment, Anhui University of Science and Technology, Huainan 232001 Anhui, China; State Key Laboratory of Mining Response and Disaster Prevention and Control in Deep Coal Mines, Anhui University of Science & Technology, Huainan 232001 Anhui, China*

Shuheng Tang − *School of Energy Resource, China University of Geosciences, Beijing 100083, China; Key Laboratory of Marine Reservoir Evolution and Hydrocarbon Enrichment Mechanism, Ministry of Education, Beijing 100083, China; Key Laboratory of Strategy Evaluation for Shale Gas, Ministry of Land and Resources, Beijing 100083, China*

Songhang Zhang − *School of Energy Resource, China University of Geosciences, Beijing 100083, China; Key Laboratory of Marine Reservoir Evolution and Hydrocarbon Enrichment Mechanism, Ministry of Education, Beijing 100083, China; Key Laboratory of Strategy Evaluation for Shale Gas, Ministry of Land and Resources, Beijing 100083, China*

Zhaodong Xi − *School of Energy Resource, China University of Geosciences, Beijing 100083, China; Key Laboratory of Marine Reservoir Evolution and Hydrocarbon Enrichment Mechanism, Ministry of Education, Beijing 100083, China; Key Laboratory of Strategy Evaluation for Shale Gas, Ministry of Land and Resources, Beijing 100083, China*

Complete contact information is available at: https://pubs.acs.org/10.1021/acsomega.1c06496

Notes

The authors declare no competing financial interest.

ACKNOWLEDGMENTS

This work was supported by the Foundation of Anhui University of Science and Technology (No. xjzd2020-05),

https://doi.org/10.1021/acsomega.1c06496
ACS Omega 2022, 7, 7715−7724

the National Natural Science Foundation of China (No. 42102216), the NSFC-Shanxi Coal-based Low Carbon Joint Fund of China (No. U1910205), the Natural Science Foundation for Distinguished Young Scholars of Anhui Province (No. 1908085J14), and the National Natural Science Foundation of China (No. 41972173). We would like to acknowledge China United Coalbed Methane Corporation for providing the production well date. Special thanks are given to anonymous reviewers for their comments and suggestions.

REFERENCES

(1) Li, Y.; Wang, Z.; Tang, S.; Elsworth, D. Re-evaluating adsorbed and free methane content in coal and its ad- and desorption processes analysis. *Chem. Eng. J.* **2022**, *428*, No. 131946.
(2) Li, Y.; Yang, J.; Pan, Z.; Tong, W. Nanoscale pore structure and mechanical property analysis of coal: An insight combining AFM and SEM images. *Fuel* **2020**, *260*, No. 116352.
(3) Humez, P.; Mayer, B.; Nightingale, M.; Becker, V.; Kingston, A.; Taylor, S.; Bayegnak, G.; Millot, R.; Kloppmann, W. Redox controls on methane formation, migration and fate in shallow aquifers. *Hydrol. Earth Syst. Sci.* **2016**, *20*, 2759−2777.
(4) Li, Y.; Wang, Y.; Wang, J.; Pan, Z. Variation in permeability during CO2−CH4 displacement in coal seams: Part 1−Experimental insights. *Fuel* **2020**, *263*, No. 116666.
(5) Huang, H.; Sang, S. X.; Miao, Y.; Dong, Z. T.; Zhang, H. J. Trends of ionic concentration variations in water coproduced with coalbed methane in the Tiefa Basin. *Int. J. Coal Geol.* **2017**, *182*, 32−41.
(6) Zhang, S.; Tang, S. H.; Li, Z. C.; Guo, Q. L.; Pan, Z. J. Stable isotope characteristics of CBM co-produced water and implications for CBM development: the example of the Shizhuangnan Block in the Southern Qinshui Basin, China. *J. Nat. Gas Sci. Eng.* **2015**, *27*, 1400−1411.
(7) Milkov, A. V.; Etiope, G. Revised genetic diagrams for natural gases based on a global dataset of > 20,000 samples. *Org. Geochem.* **2018**, *125*, 109−120.
(8) Li, Y.; Tang, S. H.; Zhang, S. H.; Xi, Z. D. In situ analysis of methanogenic pathways and biogeochemical features of CBM co-produced water from the Shizhuangnan block in the southern Qinshui Basin, China. *Energy Fuels* **2020**, *34*, 5466−5475.
(9) Ni, X.; Zhao, Z.; Wang, Y. B.; Wang, L. Optimisation and application of well types for ground development of coalbed methane from no. 3 coal seam in Shizhuang south block in Qinshui basin, Shanxi province, China. *J. Pet. Sci. Eng.* **2020**, *193*, No. 107453.
(10) Chen, B.; Stuart, F. M.; Xu, S.; Gyore, D.; Liu, C. Q. Evolution of coal-bed methane in Southeast Qinshui Basin, China: Insights from stable and noble gas isotopes. *Chem. Geol.* **2019**, *529*, No. 119298.
(11) Tao, S.; Pan, Z. J.; Tang, S. L.; Chen, S. D. Current status and geological conditions for the applicability of CBM drilling technologies in China: a review. *Int. J. Coal Geol.* **2019**, *202*, 95−108.
(12) Guo, H.; Zhang, Y. W.; Zhang, J. L.; Huang, Z. X.; Urynowicz, M. A.; Liang, W. G.; Han, Z. Y.; Liu, J. Characterization of anthracite-degrading methanogenic microflora enriched from Qinshui Basin in China. *Energy Fuels* **2019**, *33*, 6380−6389.
(13) Zhang, S.; Tang, S. H.; Li, Z. C.; Pan, Z. J.; Shi, W. Study of hydrochemical characteristics of CBM co-produced water of the Shizhuangnan Block in the Southern Qinshui Basin, China, on its implication of CBM development. *Int. J. Coal Geol.* **2016**, *159*, 169−182.
(14) Li, Y.; Tang, S. H.; Zhang, S. H.; Xi, Z. D.; Wang, P. F. Biogeochemistry and Water-Rock Interactions of Coalbed Methane Co-Produced Water in the Shizhuangnan Block of the Southern Qinshui Basin, China. *Water* **2020**, *12*, 130.
(15) DiGiulio, D. C.; Jackson, R. B. Impact to underground sources of drinking water and domestic wells from production well stimulation and completion practices in the Pavillion, Wyoming, Field. *Environ. Sci. Technol.* **2016**, *50*, 4524−4536.
(16) Li, Y.; Tang, D. Z.; Xu, H.; Elsworth, D.; Meng, Y. J. Geological and hydrological controls on water coproduced with coalbed methane in Liulin, eastern Ordos basin, China. *AAPG Bull.* **2015**, *99*, 207−229.
(17) Fu, H.; Tang, D. Z.; Pan, Z. J.; Yan, D. T.; Yang, S. G.; Zhuang, X. G.; Li, G. Q.; Chen, X.; Wang, G. A study of hydrogeology and its effect on coalbed methane enrichment in the southern Junggar Basin, China. *AAPG Bull.* **2019**, *103*, 189−213.
(18) Wolfe, A. L.; Wilkin, R. T. Evidence of sulfate-dependent anaerobic methane oxidation within an area impacted by coalbed methane-related gas migration. *Environ. Sci. Technol.* **2017**, *51*, 1901−1909.
(19) Li, Y.; Tang, S. H.; Zhang, S. H.; Xi, Z. D.; Wang, P. F. Biogeochemistry and the associated redox signature of co-produced water from coalbed methane wells in the Shizhuangnan block in the southern Qinshui Basin, China. *Energy Explor. Exploit.* **2020**, *38*, 1034−1053.
(20) Pohlman, J. W.; Riedel, M.; Bauer, J. E.; Canuel, E.; Paull, C. K.; Lapham, L.; Grabowski, K. S.; Coffin, R. B.; Spence, G. D. Anaerobic methane oxidation in low-organic content methane seep sediments. *Geochim. Cosmochim. Acta* **2013**, *108*, 184−201.
(21) Riedinger, N.; Formolo, M. J.; Lyons, T. W.; Henkel, S.; Beck, A.; Kasten, S. An inorganic geochemical argument for coupled anaerobic oxidation of methane and iron reduction in marine sediments. *Geobiology* **2014**, *12*, 172−181.
(22) Milucka, J.; Ferdelman, T. G.; Polerecky, L.; Franzke, D.; Wegener, G.; Schmid, M.; Lieberwirth, I.; Wagner, M.; Widdel, F.; Kuypers, M. M. M. Zero-valent sulphur is a key intermediate in marine methane oxidation. *Nature* **2012**, *491*, 541−546.
(23) Molofsky, L. J.; Connor, J. A.; Wylie, A. S.; Wagner, T.; Farhat, S. K. Evaluation of methane sources in groundwater in northeastern Pennsylvania. *Groundwater* **2013**, *51*, 333−349.
(24) Vinson, D. S.; Blair, N. E.; Martini, A. M.; Larter, S.; Orem, W. H.; McIntosh, J. C. Microbial methane from in situ biodegradation of coal and shale: a review and reevaluation of hydrogen and carbon isotope signatures. *Chem. Geol.* **2017**, *453*, 128−145.
(25) Yao, Y.; Liu, D. M.; Yan, T. T. Geological and hydrogeological controls on the accumulation of coalbed methane in the Weibei field, southeastern Ordos Basin. *Int. J. Coal Geol.* **2014**, *121*, 148−159.
(26) Bi, Z.; Zhang, J.; Park, S.; Harpalani, S.; Liang, Y. N. A formation water based nutrient recipe for potentially increasing methane release from coal in situ. *Fuel* **2017**, *209*, 498−508.
(27) Bao, Y.; Ju, Y. W.; Huang, H. P.; Yun, J. L.; Guo, C. Potential and constraints of biogenic methane generation from coals and mudstones from Huaibei coalfield, eastern China. *Energy Fuels* **2019**, *33*, 287−295.
(28) Schweitzer, H.; Ritter, D.; McIntosh, J.; Barnhart, E.; Cunningham, A. B.; Vinson, D.; Orem, W.; Fields, M. W. Changes in microbial communities and associated water and gas geochemistry across a sulfate gradient in coal beds: Powder River Basin, USA. *Geochim. Cosmochim. Acta* **2019**, *245*, 495−513.
(29) Meng, Y.; Tang, D. Z.; Xu, H.; Li, Y.; Gao, L. J. Coalbed methane produced water in China: status and environmental issues. *Environ. Sci. Pollut. Res.* **2014**, *21*, 6964−6974.
(30) Fu, H.; Tang, D. Z.; Xu, H.; Xu, T.; Chen, B. L.; Hu, P.; Yin, Z. Y.; Wu, P.; He, G. J. Geological characteristics and CBM exploration potential evaluation: a case study in the middle of the southern Junggar Basin, NW China. *J. Nat. Gas Sci. Eng.* **2016**, *30*, 557−570.
(31) Fuertez, J.; Cordoba, G.; McLennan, J. D.; Adams, D. J.; Sparks, T. D. Potential application of developed methanogenic microbial consortia for coal biogasification. *Int. J. Coal Geol.* **2018**, *188*, 165−180.
(32) Su, X.; Zhao, W. Z.; Xia, D. P. The diversity of hydrogen-producing bacteria and methanogens within an in situ coal seam. *Biotechnol. Biofuels* **2018**, *11*, No. 245.
(33) Whiticar, M. J. Carbon and hydrogen isotope systematics of bacterial formation and oxidation of methane. *Chem. Geol.* **1999**, *161*, 291−314.
(34) Beckmann, S.; Luk, A. W. S.; Gutierrez-Zamora, M. L.; Chong, N. H. H.; Thomas, T.; Lee, M.; Manefield, M. Long-term succession

https://doi.org/10.1021/acsomega.1c06496
ACS Omega 2022, 7, 7715−7724

in a coal seam microbiome during in situ biostimulation of coalbed methane generation. *ISME J.* **2019**, *13*, 632−650.
(35) Meng, Y.; Tang, D. Z.; Xu, H.; Li, C.; Li, L.; Meng, S. Z. Geological controls and coalbed methane production potential evaluation: a case study in Liulin area, eastern Ordos Basin, China. *J. Nat. Gas Sci. Eng.* **2014**, *21*, 95−111.
(36) Qin, Y.; Moore, T. A.; Shen, J.; Yang, Z. B.; Shen, Y. L.; Wang, G. Resources and geology of coalbed methane in China: a review. *Int. Geol. Rev.* **2018**, *60*, 777−812.
(37) Guo, C.; Qin, Y.; Han, D. Interlayer interference analysis based on trace elements in water produced from coalbed methane wells: a case study of the Upper Permian coal-bearing strata, Bide−Santang Basin, western Guizhou, China. *Arabian J. Geosci.* **2017**, *10*, No. 137.
(38) Stewart, B. W.; Capo, R. C.; Hedin, B. C.; Hedin, R. S. Rare earth element resources in coal mine drainage and treatment precipitates in the Appalachian Basin, USA. *Int. J. Coal Geol.* **2017**, *169*, 28−39.
(39) Li, Y.; Shi, W.; Tang, S. H. Microbial geochemical characteristics of the coalbed methane in the Shizhuangnan block of Qinshui Basin, north China and their geological implications. *Acta Geol. Sin.* **2019**, *93*, 660−674.
(40) Zhang, Z.; Qin, Y.; Bai, J. P.; Li, G. Q.; Zhuang, X. G.; Wang, X. M. Hydrogeochemistry characteristics of produced waters from CBM wells in Southern Qinshui Basin and implications for CBM commingled development. *J. Nat. Gas Sci. Eng.* **2018**, *56*, 428−443.
(41) Baublys, K. A.; Hamilton, S. K.; Golding, S. D.; Vink, S.; Esterle, J. Microbial controls on the origin and evolution of coal seam gases and production waters of the Walloon Subgroup; Surat Basin, Australia. *Int. J. Coal Geol.* **2015**, *147−148*, 85−104.
(42) Zhang, Z.; Qin, Y. A preliminary investigation on water quality of coalbed natural gas produced water for beneficial uses: a case study in the Southern Qinshui Basin, North China. *Environ. Sci. Pollut. Res.* **2018**, *25*, 21589−21604.

https://doi.org/10.1021/acsomega.1c06496
ACS Omega 2022, 7, 7715−7724